

Mechanical properties of interfacial phases between Sn-3.5 Ag solder and Ni-18 at. % W barrier film by nanoindentation

C.S. Chew and R. Durairaj

Department of Mechanical and Materials Engineering, University Tunku Abdul Rahman, Kuala Lumpur, Malaysia,

A.S.M.A. Haseeb

Department of Mechanical Engineering, University of Malaya, Kuala Lumpur, Malaysia, and

B. Beake

Micro Materials Ltd., Wrexham, UK

Abstract

Purpose – The purpose of this paper is to investigate the hardness and elastic modulus on interfacial phases formed between Sn-3.5Ag solder and Ni-18 at. % W alloy film by nanoindentation. It has been found that a ternary amorphous Sn-Ni-W layer formed below Ni₃Sn₄ IMC at the interface. In this study, mechanical properties of the IMC formed between SA solder and Ni-18 at. % W film after six times reflows were performed by nanoindentation.

Design/methodology/approach – The characterization was carried at 25°C, and 100 indents were generated. The elastic modulus and hardness were investigated.

Findings – The results showed that hardness of Ni₃Sn₄ IMC was higher than amorphous Sn-Ni-W phase. A slight bigger indent was observed on the Sn-Ni-W layer compared with that on the Ni₃Sn₄ IMC. Lower topographical height in the Sn-Ni-W layer indicated that the Sn-Ni-W phase was softer compared with the Ni₃Sn₄ IMC. The lower hardness and soft Sn-Ni-W phase is significantly related to the amorphous structure that formed through solid-state amorphization.

Originality/value – There are no publications about the indentation on the interfacial between the Ni-W layer and the Sn-Ag solder.

Keywords Intermetallic compounds, Microstructure, Reflow soldering, Coatings

Paper type Research paper

1. Introduction

Tin-based solders have been given lots of attention as replacements for lead-based solders in recent years. In microelectronic packaging, copper comes into contact with lead-free solder and the tin reacts with the copper to form Cu-Sn intermetallic compounds (IMC). These brittle compounds continue to grow and degrade the lifetime of the solder joint after multiple reflows and lengthy aging. Nickel films have been introduced to slow down the interfacial reaction between the lead-free solder and the copper substrate. Alloying elements have been added into the nickel-based barrier layer to stabilize its film. Among them, B, Co, P, W and V alloying elements have received the most attention (Jeong-Won *et al.*, 2010; Ho *et al.*, 2013; Yang *et al.*, 2013; Awe and Oshakuade, 2014; Yang *et al.*, 2014).

At the interface between the Sn-3.5 Ag solder (SA) and a Ni-P film, two P-rich layers, Ni₃P and nanocrystalline Ni-Sn-P were found below the Ni₃Sn₄ IMC after prolonged soldering (Sharif and Chan, 2005; Wu *et al.*, 2009; Wu *et al.*, 2010). The

nanocrystalline Ni-Sn-P layer and Ni₃P layer have been found to be brittle (Wu *et al.*, 2009; Kim and Pak, 2010; Wu *et al.*, 2010). Shmyreva revealed that nanocrystalline layers possessed high strength and high hardness. In contrast, amorphous metallic materials have higher plasticity than nanomaterials, because of the absence of the crystalline lattice (Kim and Pak, 2010).

In previous studies, a Sn-Ni-W ternary phase was observed below the Ni₃Sn₄ layer at the SA and Ni-W alloy film interface (Haseeb *et al.*, 2011). The ternary phase was found to be an amorphous layer formed through solid-state amorphization caused by anomalously fast diffusion of Sn into the Ni-W film. This finding is similar to the case for a Ni-V film, where an amorphous ternary phase, Ni-Sn-V, was formed between the Ni₃Sn₄ IMC and the Ni-V film after soldering (Chen and Chen, 2006). Yet, there has been no study of the mechanical properties of the amorphous Ni-Sn-V layer. It was thus interesting to investigate the mechanical properties of the amorphous layer which formed by solid-state amorphization, as was performed in this study.

The current issue and full text archive of this journal is available on Emerald Insight at: www.emeraldinsight.com/0954-0911.htm



Soldering & Surface Mount Technology
27/2 (2015) 90–94
© Emerald Group Publishing Limited [ISSN 0954-0911]
[DOI 10.1108/SSMT-01-2015-0001]

The authors would like to acknowledge the financial support from Research University Grant, University of Malaya (Project no. RG 068/09AET) and Institute of Research Management and Consultancy (IPPP), University of Malaya (Project no. PS354-2009B). Special thanks to Micro Materials Ltd., UK.

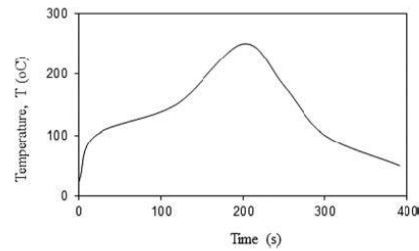
Received 6 January 2015
Revised 24 February 2015
Accepted 25 February 2015

Nanoindentation is a precise tool for examining and evaluating the mechanical properties of microelectronic materials on a small scale without destroying the samples. The machine has a good ability in measuring the mechanical properties, specifically the elastic modulus and hardness, of thin films on a substrate. A number of studies have been published on measuring the mechanical strength of IMCs which formed between lead-free solder and its substrates by nanoindentation (Gao and Takemoto, 2006; Liu and Chen, 2007; Yang *et al.*, 2008; Rosenthal *et al.*, 2010; Marques *et al.*, 2013; Xiao *et al.*, 2014). However, there is still a lack of information for certain IMCs that form between the interfaces, especially those between lead-free solder and Ni-W alloys films. To understand the mechanical properties of the ternary Sn-Ni-W layer that formed between the SA and Ni-W alloy film, nanoindentation testing was performed across the interfaces. In this paper, the hardness and elastic modulus at the interface between the electrodeposited Ni with 18 at. % W alloys films and SA solder after six reflow cycles have been investigated. This was because, in a previous study (Chew *et al.*, 2012), the Ni_3Sn_4 thickness layer was found to decrease with increasing W content in the Ni-W film; however, the thickness of the Sn-Ni-W amorphous layer was not significantly dependent on the W content in the Ni-W film. It is generally believed that the amorphous layer formed in a Ni-18 at. % W alloy film can be an effective barrier, as it exhibits low diffusivity. Such films, therefore, have the potential to provide long-term barrier properties. 2D maps of hardness and elastic modulus at each intermetallic phase are also discussed. To further understand the mechanical behavior of the IMC across the specimen, an atomic force microscope (AFM) was also used for supporting analysis.

2. Experimental procedure

Sn-3.5Ag (SA) lead-free solder paste (Indium Corporation of America, Singapore) was used in this study. Ni-W alloy films were prepared on a clean copper substrate by electrodeposition. The composition and parametric details were as listed in previous papers (Chew *et al.*, 2009; Chew *et al.*, 2010; Haseeb *et al.*, 2011; Chew *et al.*, 2012). The tungsten content of the bath was controlled to deposit Ni with 18 at. % W. Before soldering, the film was cleaned with detergent, rinsed thoroughly in deionized water and dried with acetone. The solder paste was placed on the Ni-18 at. % W electrodeposited substrate through a mask with a 6.5-mm opening and 1.24 mm height. Soldering was conducted via six reflow cycles and a peak temperature of 250°C in an oven (forced convection, FT 02, CIF). The reflow temperature profile is shown in Figure 1. After the reflow process, the sample was cooled to room temperature. The flux residue on the top of the solder was cleaned using acetone. The sample was then cut by using a diamond saw and prepared for cross-sectional examination using standard metallographic techniques. The microstructure was studied using a field emission scanning electron microscope (Gemini field emission scanning electron microscope (FESEM), Zeiss). The elemental analysis of the IMC was carried using an energy-dispersive X-ray spectroscopy (EDX). The surface topographical analysis was performed before indentation with an AFM (AFM, Veeco).

Figure 1 Temperature profile of reflowing process



The mechanical properties were determined by a nanoindenter (Micro Materials, Wrexham, UK) using a Berkovich tip. The tests were carried out at 25 °C. Indentation tests were performed across the solder–substrate interface using a peak load of 0.5 mN at a load/unload rate of 0.025 mN/s. A grid (10 × 10) programmed as 100 indentations with a 2- μm indent spacing and an angled grid (15 × 25) as 375 indentations with a 1- μm indent spacing were used. Hardness and reduced elastic modulus were defined for different intermetallic phases. The location of the indentations was confirmed by FESEM.

3. Results and discussion

Figure 2 shows a cross-sectional FESEM micrograph of the interface between SA and Ni-18 at. % W film after six reflows. Two reaction phases were formed at the solder joint interface.

A uniform and well-faceted IMC was observed between the SA and Ni-18 at. % W film. Elemental analysis obtained by EDX confirmed that the faceted IMC was Ni_3Sn_4 . A bright layer and a continuous layer grew below the Ni_3Sn_4 IMC. The bright layer consisted of the elements Sn, W and Ni. In a previous study, the bright layer was found to be an amorphous structure (Haseeb *et al.*, 2011). It was suggested that the bright layer formed through solid-state amorphization caused by the anomalously fast diffusion of Sn into the Ni-W film.

Figure 2 Cross-sectional back scatter electron micrograph of the interface between SA and Ni-18 at. % W after six reflow cycles

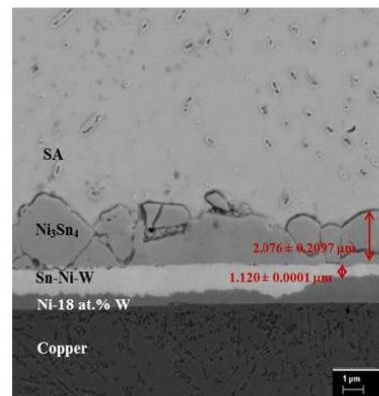


Figure 3 a) AFM topography image at the interface between SA and Ni-18 at % W after six reflows; b) Depth profile across the interface of IMC as a function of distance across the sample surface

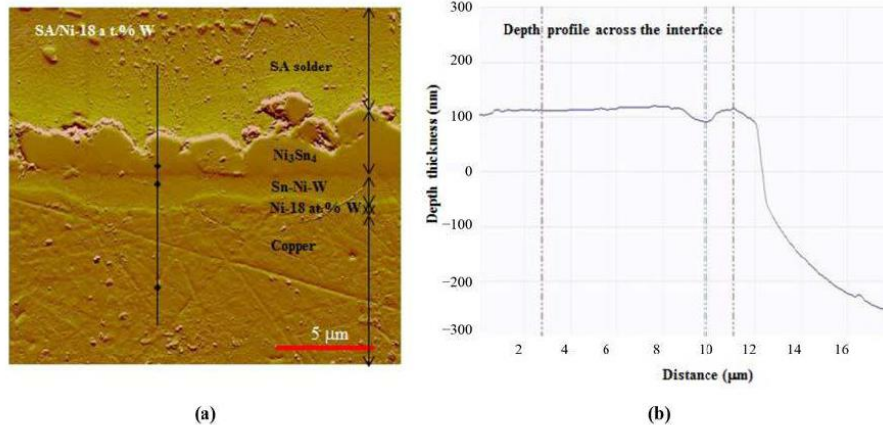
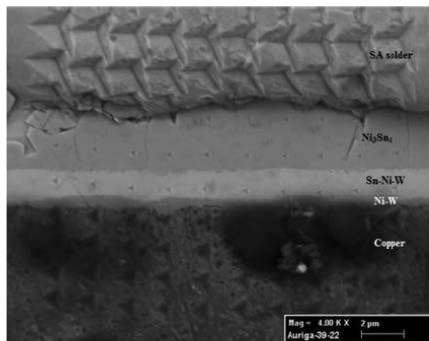


Figure 3(a) shows an AFM topography image of the interface between the SA and Ni-18 at % W. The topographical height across the sample surface is displayed in Figure 3(b). In the copper region, the topographical height remains constant more or less until it reaches the Sn-Ni-W phase. A drop in height is observed in the Sn-Ni-W phase, while a slight rise is seen in the Ni_3Sn_4 phase. A sudden fall in height is found in the SA solder region. The lower topographical height in the Sn-Ni-W qualitatively suggests that the Sn-Ni-W phase was softer compared with the Ni_3Sn_4 . It is suggested that during metallographic polishing of the Sn-Ni-W layer, the softer layer was worn out at a faster rate, which led to the formation of a depression at the Sn-Ni-W, as observed in the figure.

To measure the mechanical properties of the phases at the interfacial region, nanoindentation was performed covering all the interfacial phases. Figure 4 shows the FESEM micrograph of the indents at the interface between the SA and Ni-18 at % W. It can be seen that the largest indents were observed at the solder matrix. Much smaller indents were found on both

Figure 4 FE-SEM image of indents across the interface between SA and Ni-18 at % W



the Ni_3Sn_4 and Sn-Ni-W phases. The indents on the Sn-Ni-W phase appear larger compared with those on the Ni_3Sn_4 . The hardness, H, and reduced elastic modulus, E, of the phases across the interface calculated from the indentation data are shown in Table I. The Ni_3Sn_4 has a hardness and modulus of 6.79 GPa and 134.24 GPa, respectively. Table II displays the literature data for the Ni_3Sn_4 IMC. The bright layer, Sn-Ni-W, is softer and has a hardness and modulus of H = 4.10 GPa and E = 128.834 GPa, respectively. The hardness of the Sn-Ni-W is seen to be lower than that of Ni_3Sn_4 .

Figure 5(a and b) displays the 2D maps at the solder-substrate interface of hardness and elastic modulus. It is clearly indicated that across the SA, Ni-W film and copper substrate region, various hardness and elastic moduli at each intermetallic phase can be seen. Some variation of hardness in

Table I Hardness and elastic modulus of intermetallic phases at SA interface

Intermetallic phase	Elastic modulus (GPa)	Hardness (GPa)
SA	76.29 ± 2.90	0.29 ± 0.02
Ni_3Sn_4	134.24 ± 13.60	6.79 ± 0.60
Sn-Ni-W	128.834 ± 28.68	4.10 ± 1.67
Cu	152.16 ± 11.69	1.70 ± 0.03

Table II Data obtained from the literature values for the hardness and elastic modulus of the Ni_3Sn_4 intermetallic phase

Intermetallic phase	Hardness (GPa)	Elastic modulus (GPa)	Reference
Ni_3Sn_4	6.79 ± 0.598	134.24 ± 13.602	Current study
		152	Tsai <i>et al.</i> (2006)
		130-150	(Xu and Pang 2006)
	8.12 ± 0.62	140.4 ± 7.9	Jang <i>et al.</i> (2004)
	6.31 ± 0.16	141.12 ± 3.85	Yang <i>et al.</i> (2008)
	4.8	152	Albrecht <i>et al.</i> (2003)
	6.1 to 7.0	119.4 to 134.0	Chen <i>et al.</i> (2006)
	6.33		Yang <i>et al.</i> (2009)

Link to Full-Text Articles :

<http://www.emeraldinsight.com/doi/full/10.1108/SSMT-01-2015-0001>